Chapter 33. Three-dimensional spectroscopy of vibrational energy relaxation in liquids

CONFERENCE PAPER · JULY 2003

DOI: 10.1016/B978-044451656-5/50033-5

4 AUTHORS:

Zhaohui Wang

Xiamen University

34 PUBLICATIONS **1,066** CITATIONS

SEE PROFILE

Andrei V. Pakoulev

University of Wisconsin–Madison

36 PUBLICATIONS **620** CITATIONS

SEE PROFILE

Yoonsoo Pang

Gwangju Institute of Science and Technology

28 PUBLICATIONS **528** CITATIONS

SEE PROFILE

Dana D Dlott

University of Illinois, Urbana-Champaign

297 PUBLICATIONS **6,640** CITATIONS

SEE PROFILE

Ultrafast Events in Molecular Science, eds. by M. Martin and J. T. Hynes (Amsterdam, Elsevier, 2004)

Three-dimensional spectroscopy of vibrational energy relaxation in liquids.

Zhaohui Wang, Andrei Pakoulev, Yoonsoo Pang and Dana D. Dlott*

School of Chemical Sciences, University of Illinois at Urbana-Champaign, 600 S. Mathews Ave., Urbana, IL 61801

ABSTRACT

A three-dimensional vibrational spectroscopy technique with mid-IR pumping and incoherent anti-Stokes Raman probing is used to study vibrational energy relaxation (VR) in hydrogen-bonded liquids. New results on spectral diffusion and vibrational relaxation of OH stretching ν_{OH} of water are presented. Vibrational energy transfer down a molecular chain is probed with angstrom spatial resolution in a series of alcohols where ν_{OH} is pumped and energy transfer through methylene -CH_2- to terminal methyl -CH_3 groups is probed.

1. INTRODUCTION

Vibrational energy relaxation (VR) in liquids is a fundamental process in chemical physics that remains poorly understood. When a parent vibration is excited, it typically decays on the picosecond time scale. In polyatomic molecules with many vibrational states, excitation of a higher frequency parent vibration leads to a complicated chain of events termed vibrational cooling (VC). In VC, parent decay could excite one or more daughter vibrations. The leftover energy is transferred to collective excitations of the liquid [1]. Ultimately all the daughter and higher energy collective excitations will decay in secondary processes resulting In a bulk increase in the thermodynamic temperature by an amount ΔT [2-4]. In the past several years, a number of multidimensional vibrational spectroscopy techniques have been used to study liquids. Most of these techniques involve vibrational coherences, so they are of limited use in probing VR. Although coherence decays can sometimes be related to population relaxation, successive generation of daughter vibrations is essentially impossible to observe with a coherent probe. In the 1970's, Laubereau and Kaiser combined picosecond mid-IR excitation with an incoherent anti-Stokes Raman probe [5]. With the lasers available at that time, they could study the decay of parent CH and OH stretching transitions ν_{OH} and ν_{CH} of several liquids and in certain cases observe a few of the daughter vibrations [6]. In our laboratory we have developed a powerful spectrometer based on a 1 ps amplified Ti:sapphire laser system with dual optical parametric amplifiers. This spectrometer produces a powerful mid-IR pump pulse tunable in the 3700-2200 cm^{-1} range, plus a fixed 532 nm probe pulse. The combination of a tunable pump pulse and multichannel detection of the incoherent anti-Stokes spectrum leads to an important type of 3D vibrational spectroscopy [7]. The three dimensions are the pump wavenumber, the probe wavenumber and time. In this paper, we

* Author to whom correspondence should be addressed. Electronic mail dlott@scs.uiuc.edu

discuss two problems studied with 3D vibrational spectroscopy: (1) VR and spectral diffusion in water, and (2) vibrational energy transfer within molecules probed with angstrom spatial resolution.

2. WATER STUDIES

Water is an interesting and important liquid. As the combination of multidimensional vibrational spectroscopy and molecular dynamics helps us understand water better, more and more complex dynamics have been revealed [8,9]. We can briefly explain why a liquid of triatomic molecules turns out to be so immensely complicated: *Water's three atoms bestow all the complexity of multiple intramolecular vibrations, and in addition in water there are more hydrogen bonds (~3.57) than atoms!*

Multidimensional spectroscopy of ν_{OH} provides new information about spectral diffusion and VR. With a few exceptions [3,4], most experiments have concentrated on dilute solutions of the HOD molecule in D_2O (reviewed in ref. [10]). Our recent work has focused on water itself. Although one might expect ν_{OH} hydrogen bond dynamics to be similar in HOD/D_2O and water, VR is entirely different. Figure 1 is a schematic of the energy levels for ν_{OH} VR in HOD/D_2O and in water. There are seven VR pathways for ν_{OH} of HOD/D_2O [10], but only two in water [11]. The two water ν_{OH} VR pathways are $\nu_{OH} \rightarrow \delta_{H2O}$ (~1700 cm^{-1}) and $\nu_{OH} \rightarrow$ ground state (~3350 cm^{-1}), where δ_{H2O} is the water bending vibration near 1640 cm^{-1}, and the values in parentheses indicate the amount of energy deposited into the collective vibrations of the liquid. Back in 2000, our group studied VR of HOD/D_2O with ν_{OH} pumping [12]. To illustrate the complexities of VR in this system, Fig. 2 shows some IR-Raman data. We have directly observed the decay of the parent and the appearance and decay of three daughter vibrations, $\nu_{OD}(D_2O)$, δ_{HDO} and δ_{D2O}.

It is now generally accepted that spectral diffusion in ν_{OH} on the >100 fs time scale is caused largely by the making and breaking of hydrogen bonds [8,9]. One important question about hydrogen bond dynamics involves the multicomponent vs. continuous environment

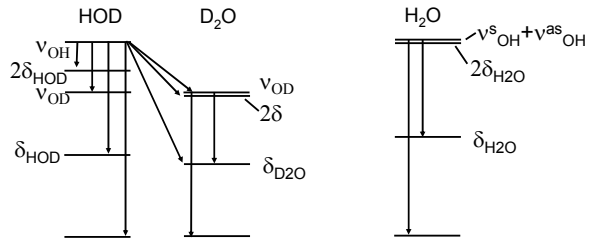

Fig. 1. Vibrational relaxation (VR) pathways of ν_{OH} of HOD in D_2O and of ν_{OH} of water. For HOD there are four intramolecular pathways and three intermolecular pathways to the D_2O solvent. For water, there are only two pathways, although the daughter δ_{H2O} might be located on the same or on an adjacent molecule. In each pathway the leftover energy appears as excitations of lower frequency collective modes of the liquid.

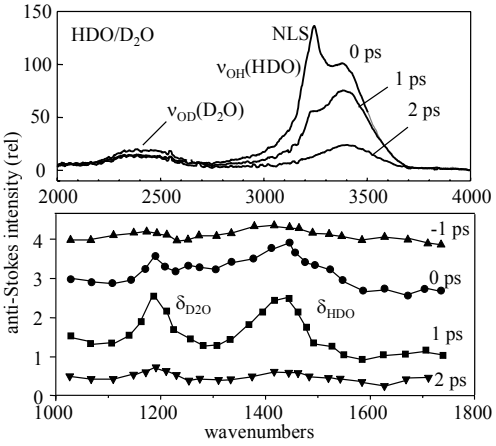

Fig. 2. Anti-Stokes Raman transients for HDO in D_2O. NLS is an artifact produced by nonlinear light scattering. The spectra in the bending region are offset for clarity. Reproduced from ref. [12].

question. In theoretical simulations of water hydrogen bonding, there are broad distributions of the O-H···O bond angles and lengths, suggesting continuously varying environments. Theorists often define hydrogen bonds as "made" or "broken" based on certain sharp cut-off criteria for the O-H···O bond angles and lengths, making it possible to count the number of hydrogen bonds at each simulated water molecules (the average number is 3.57), so that well-defined hydrogen bonding environments with 4, 3, 2 or even fewer bonds can be identified. Recent work by the groups of Casey Hynes and Jim Skinner [8,9] show that the ν_{OH} spectrum of different hydrogen-bonded configurations are distinguishable, but they overlap a great deal. Due to this overlap, it is not possible to resolve individual environments with ordinary vibrational spectroscopy. Laenen and Laubereau [13,14] studied HOD/D_2O with two-color pump-probe techniques and concluded there were at least three well-defined subbands in the ν_{OH} spectra. On the basis of comparisons to simulations, these bands were assigned to (I) "ice-like", (II) "bridged" and (III) "bifurcated" hydrogen bonded sites. Laenen argued that the subband method of analysis made more sense than looking at transients at individual probe wavelengths because single-wavelength transients always contain a mixture of spectral diffusion and VR. In subsequent work in other laboratories on HOD/D_2O, the discrete environment picture was ignored in favor of a continuous distribution picture, where ν_{OH} dynamics were explained in terms of spectral diffusion plus a wavenumber-dependent VR lifetime [15].

Some IR-Raman data on water with ν_{OH} pumping at 3115 cm^{-1} are shown in Fig. 3. The decay of ν_{OH} and the appearance of δ_{H2O} are clearly seen. Figure 4 compares the equilibrium Stokes Raman spectrum of ν_{OH} to transient anti-Stokes spectra at t = 1 ps with pumping on the red edge, the band center and the blue edge. The transient spectra can be accurately fit at all times and all pump wavenumbers with two overlapping Gaussian vibrational subbands [16], a broader (FWHM ≈ 500 cm^{-1}) red-shifted subband and a narrower (FWHM ≈ 200 cm^{-1}) blue-shifted subband. The amplitudes, peak locations and widths of these two subbands vary with time, but each subband has a well-defined lifetime T_1. The time dependences of the ν_{OH} subband intensities and the daughter δ_{H2O} bending vibration are

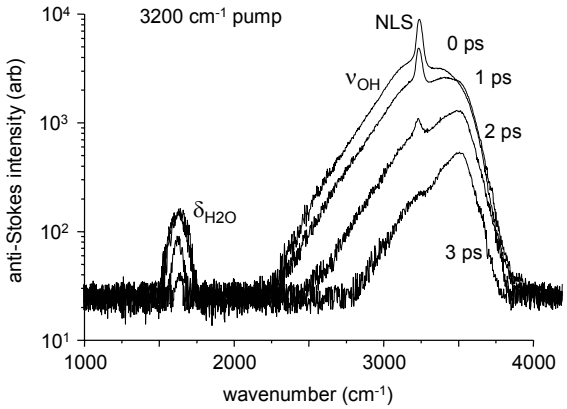

Fig. 3. Anti-Stokes transient spectra of water with ν_{OH} pumping at 3200 cm^{-1}. The sharp feature at 3200 cm^{-1} is due to nonlinear light scattering (NLS). The blueshift with increasing time is due to spectral diffusion and a longer lifetime in the blue. Reproduced from ref. [11].

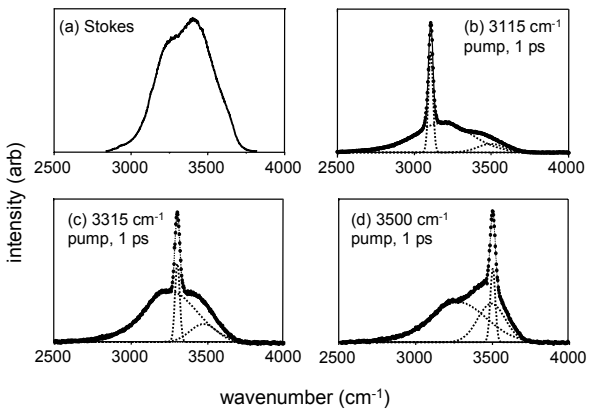

Fig. 4. (a) Stokes Raman spectrum of water. (b)-(d) Anti-Stokes transients after pumping on the red edge, band center and blue edge. The data are fit by the sum of two overlapping Gaussian subbands plus one Gaussian for the NLS artifact. Reproduced from ref. [16].

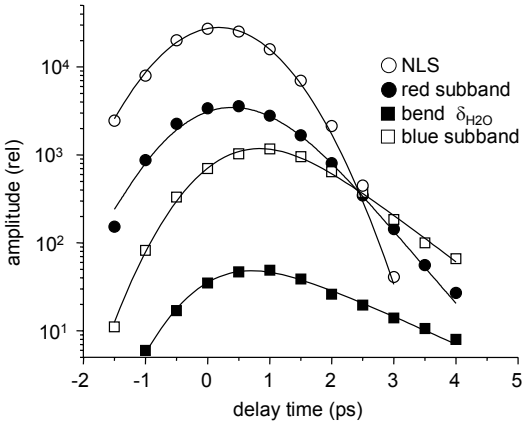

Fig. 5. Time dependence of the red and blue subbands and δ_{H2O} with 3115 cm^{-1} pumping. The NLS artifact gives the apparatus time response. Reproduced from ref. [11].

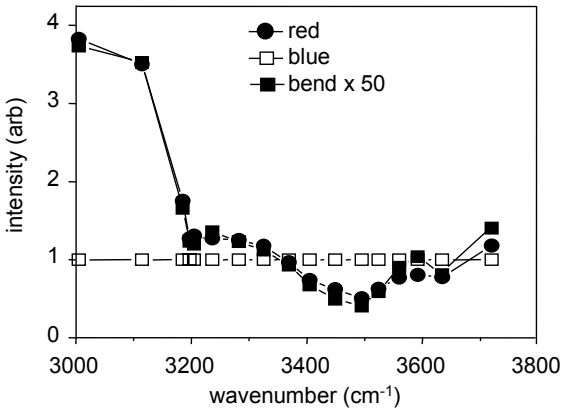

Fig. 6. Relative intensities of red and blue subbands and δ_{H2O} as a function of pump wavenumber, normalized to the blue subband intensity. The δ_{H2O} intensities are multiplied by 50. Reproduced from ref. [11].

shown in Fig. 5. The red subband, which is directly excited by the 3115 cm^{-1} pump pulse, rises instantaneously. The red subband data were fit with the convolution of the apparatus response measured via nonlinear light scattering (NLS) plus an exponential decay, giving T_1 = 0.55 ± 0.05 ps. The blue subband, not directly pumped by 3115 cm^{-1} pulses, has a delayed rise. Those data were fit by the convolution of the apparatus response with a 0.55 ps exponential build up and an exponential decay giving T_1 = 0.75 ± 0.05 ps. The bend vibration δ_{H2O} showed a delayed build up, so the signals were fit with a 0.55 ps build up and an exponential decay. The best fit for the δ_{H2O} lifetime was T_1 = 1.4 (±0.2) ps.

With anti-Stokes probing it is possible to determine the absolute quantum yield for generation of daughter δ_{H2O} by parent ν_{OH} decay [11]. The quantum yield is found from the ratio of anti-Stokes intensities and the ratio of Raman cross-sections obtained from the Stokes spectrum. In water this is complicated by having two parent subbands. Figure 6 shows how the δ_{H2O} intensity changes as the pump wavenumber is tuned through the ν_{OH} absorption. In Fig. 6, we normalized the signal at each pump wavenumber to the blue subband intensity to account for variations in laser parameters and sample absorption. In this format the blue subband intensity remains constant while the red subband and bend intensities change by a factor of ~8 as the pump wavenumber is tuned. Figure 6 shows that the bend intensity is highly correlated with the red subband and apparently uncorrelated with the blue subband. Thus δ_{H2O} is primarily generated by red subband decay, and blue subband decay creates little or no δ_{OH}. The quantum yield for stretch-to-bend is ϕ = 0.33 (±0.05) for the red subband and $\phi \approx 0$ for the blue subband. Thus,

ν_{OH} (red subband) $\rightarrow$ δ_{H2O} (1/3) + ground state (2/3).

ν_{OH} (blue subband) $\rightarrow$ ground state.

In conclusion, the water ν_{OH} Raman spectrum can be explained with two overlapping subbands. Even though these subbands overlap, they are easily distinguished with 3D vibrational spectroscopy, since they have different spectral diffusion, different lifetimes and

different VR pathways. However 3D spectroscopy does not unambiguously identify the nature of the subbands. The properties of the smaller blue subband, namely a narrower width, a longer lifetime, weaker coupling to the bending vibration and higher temperature sensitivity suggest that it represents water molecules with a broken hydrogen bond to one H atom, although this tentative structural interpretation needs to be confirmed by simulations.

3. WATCHING VIBRATIONAL ENERGY WITH ANGSTROM RESOLUTION

We have for the first time directly observed vibrational energy transfer (VET) across molecules of different lengths using vibrational reporter groups (atomic groups with nearly local-mode vibrational excitations) [17]. The distances between vibrational donors and acceptors were varied in units of one carbon-carbon bond length (~1.5 Å), so that the distance-dependence of VET could be investigated. We studied a series of different alcohols at ambient temperature, that have the general structure CH_3-R-OH, where R is a hydrocarbon. Using the IR-Raman technique, ν_{OH} was pumped and ν_{CH} transitions were probed. Although IR-Raman and related IR-IR techniques [18-22] have been used to study ethanol and other alcohols in the past, prior studies have not had the time resolution and sensitivity needed to observe the distance dependence of VET across molecular dimensions.

We stress that VET from ν_{OH} to ν_{CH} of alcohol molecules is not an efficient process. Both types of excitations have short VR lifetimes of about 1 ps, which result from decay to daughters including OH and CH bending and CO stretching in the 1000-1500 cm^{-1} range [23]. Owing to these short lifetimes, VR competes effectively with VET, so that at most a few percent of the initial OH stretch excitation makes its way down a molecular chain.

Although VET from a vibrational donor to an acceptor on another part of a molecule seems reminiscent of electronic energy transfer between dye molecules, it is fundamentally quite different. Electronic energy transfer typically results from through-space interactions, such as a dipole-dipole interaction in the case of Förster transfer, between electronic states of molecules with overlapping emission and absorption spectra. Through-space VET is not expected to be significant between ν_{OH} and ν_{CH} located a few angstroms apart, because typical dipole moments and spectral overlap factors for vibrational transitions do not provide energy transfer rates that are remotely competitive with the VR lifetimes. Instead VET is fundamentally mechanical, and occurs via a through-bond interaction involving solvent-assisted anharmonic coupling [1].

Broadly speaking, we can envision two different paradigms for excitation energy to be transferred from OH o a terminal CH_3, as shown in Fig. 7. In a *vibrational cascade*, vibrational excitation percolates down the energy levels. If this mode were dominant, Fig. 7 shows that ν_{OH} decay would first excite the higher energy "*a*" states $\nu_a(CH_3)$ and $\nu_a(CH_2)$, followed by the lower energy "*s*" states $\nu_s(CH_2)$ and $\nu_s(CH_3)$. ($\nu_a(CH_2)$ is not shown explicitly in Fig. 7 because this transition is not seen in the Raman or IR spectra of these alcohols). In *through-bond transfer*, vibrational excitation would run from OH across the intervening C-H groups, first to CH_2 and then to CH_3. Figure 7 shows that energetically this involves *a first step down in energy* from ν_{OH} to $\nu_s(CH_2)$, followed by *steps up in energy* to $\nu_s(CH_3)$ and $\nu_a(CH_3)$. Keep in mind that in our studies of ambient liquids, $k_BT \approx 200$ cm^{-1}, so steps up or down in energy of this magnitude are facile.

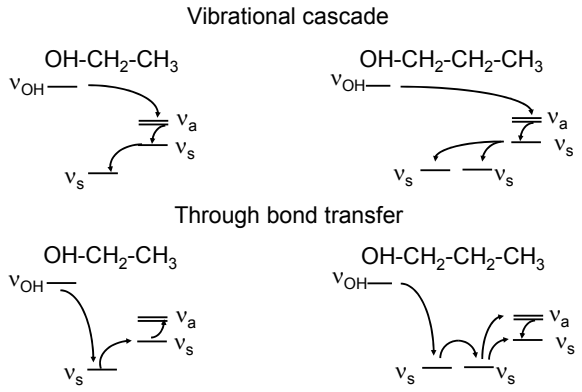

Fig. 7. Energy level diagrams for possible vibrational energy transfer (VET) processes from OH to CH stretching of ethanol and 1-propanol. (*top*) Vibrational cascade moves down in energy in each step (*bottom*) Through-bond VET moves first down then up in energy. Reproduced from ref. [17].

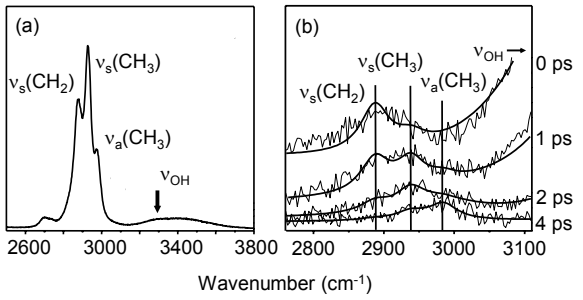

Fig. 8. (a) Stokes spectrum of ethanol. (b) Anti-Stokes transient spectra. The OH excitations pumped by the laser are cut off to the right. Vibrational energy first flows downhill from OH to CH_2, then later moves uphill in energy to CH_3, indicating through-bond vibrational energy transfer. Reproduced from ref. [17].

The Stokes Raman spectrum of ethanol in Fig. 8a shows that we can clearly resolve the OH stretch and the CH stretch of methylene and methyl. Note the Raman cross-section for ν_{OH} is about ten times smaller than for ν_{CH}. The anti-Stokes transient spectra in Fig. 8b were obtained with ν_{OH} pumping at 3300 cm^{-1}. At shorter delay times, the ν_{OH} intensity (cut off at the right hand side) is about ten times larger than the ν_{CH} intensity. Given the relative cross-sections, we see that only a few percent of ν_{OH} is transferred to ν_{CH}. The rest disappear into lower energy states [23]. In the first 1 ps, the predominant daughter of ν_{OH} decay in the ν_{CH} region is the methylene stretch $\nu_s(CH_2)$. Subsequently the energy in the methylene group does something apparently startling. It moves *uphill in energy* from $\nu(CH_2)$ to $\nu(CH_3)$. Thus the data in Fig. 8b clearly distinguish between the two possibilities illustrated in Fig. 7. Energy transfer from ν_{OH} to $\nu(CH_3)$ in ethanol *occurs by through-bond transfer*, moving from OH first to CH_2 before arriving at CH_3, as opposed to a vibrational cascade down the energy levels from OH to CH_3 to CH_2.

Figure 9 shows the time dependence of the OH and CH stretches of methylene and terminal methyl groups in ethanol, 1-propanol, 1-butanol and 2-propanol. The vertical markers in each panel indicate the peak of the OH population and the 95% point of the CH_3(a) population. The time interval between the markers for ethanol is 1.0 ps, for 1-propanol it is 1.4 ps and for 1-butanol it is 1.7 ps. Thus to a rough approximation, adding an additional methylene group increases the time for vibrational flow from one end of an alcohol molecule to the other by ~0.4 ps. In 2-propanol, energy flowing from OH to a terminal methyl passes through only a single intervening CH atomic group. The markers in Fig. 9d show the time for energy flow from OH to CH_3 in 2-propanol is almost exactly the same as in ethanol, 1.0 ps. The efficiency of energy transfer through CH in 2-propanol, where the intervening group has only one CH stretch excitation, is about one-third the efficiency of energy transfer through CH_2 in ethanol, where the intervening group has two CH stretch excitations.

Carbon-carbon bond lengths in unsaturated molecules are typically 0.15 nm, so a 0.4 ps time constant for VET across a methylene group roughly corresponds to a velocity of 375

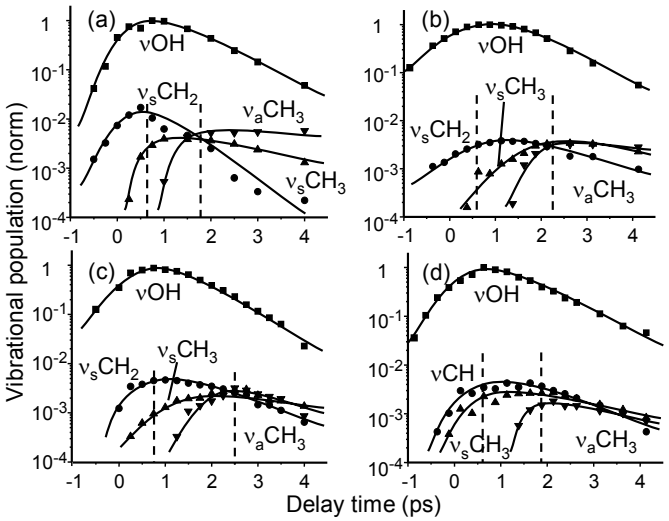

Fig. 9. Time-dependent populations of OH and CH stretching of (a) ethanol, (b) 1-propanol, (c) 1-butanol and (d) 2-propanol. The dashed vertical lines indicate the peak of the ν_{OH} population and the 95% point of the $\nu_a CH_3$ population. Reproduced from ref. [17].

m/s. That is a relatively high velocity, about ten percent greater than Mach 1. However it is only about one-third the speed of sound in ethanol. The overall efficiency for VET from OH to $\nu_a(CH_3)$ states is quite poor, so it will be interesting if we can find other useful vibrational reporter groups with longer lifetimes, and intervening groups that are better conductors of vibrational energy, so our studies could be extended to larger molecules and longer distances.

4. CONCLUSION

The 3D IR-Raman technique provides a wealth of new information about incoherent VR processes of molecules in liquids. In particular, the ability to simultaneously probe both parent and daughter vibrations proved immensely useful. The main drawback of this technique is the difficulty in observing the weak incoherent signal against a variety of possible optical backgrounds generated by the intense pump and probe pulses. Besides continuing our explorations of water and VET with high spatial resolution, future work in our lab will involve developing methods to study the temperature dependence in liquids and to study solids at low temperature.

5. ACKNOWLEDGEMENT

This material is based on work supported by the National Science Foundation under award number DMR-0096466, by Air Force Office of Scientific Research contract F49620-03-1-0032, and by Army Research Office contract DAAD19-00-1-0036.

REFERENCES

[1] V. M. Kenkre, A. Tokmakoff, and M. D. Fayer, J. Chem. Phys. 101 (1994) 10618.
[2] L. K. Iwaki, J. C. Deàk, S. T. Rhea, and D. D. Dlott, in: Ultrafast Infrared and Raman Spectroscopy, eds. M. D. Fayer (Marcel Dekker, New York, 2000).
[3] A. J. Lock, S. Woutersen, and H. J. Bakker, J. Phys. Chem. A 105 (2001) 1238.
[4] A. J. Lock and H. J. Bakker, J. Chem. Phys. 117 (2002) 1708.
[5] A. Laubereau and W. Kaiser, Rev. Mod. Phys. 50 (1978) 607.

[6] A. Seilmeier and W. Kaiser, in: Ultrashort Laser Pulses and Applications, Vol. 60, eds. W. Kaiser (Springer Verlag, Berlin, 1988), p. 279.
[7] D. D. Dlott, Chem. Phys. 266 (2001) 149.
[8] C. P. Lawrence and J. L. Skinner, Chem. Phys. Lett. 369 (2003) 472.
[9] R. Rey, K. B. Møller, and J. T. Hynes, J. Phys. Chem. A 106 (2002) 11993
[10] C. P. Lawrence and J. L. Skinner, J. Chem. Phys. 119 (2003) 1623.
[11] A. Pakoulev, Z. Wang, Y. Pang, and D. D. Dlott, Chem. Phys. Lett. in press (2003).
[12] J. C. Deàk, L. K. Iwaki, and D. D. Dlott, J. Phys. Chem. 104 (2000) 4866.
[13] R. Laenen, C. Rauscher, and A. Laubereau, Phys. Rev. Lett. 80 (1998) 2622.
[14] R. Laenen, C. Rauscher, and A. Laubereau, J. Phys. Chem. B 102 (1998) 9304.
[15] G. M. Gale, G. Gallot, and N. Lascoux, Chem. Phys. Lett. 311 (1999) 123.
[16] Z. Wang, A. Pakoulev, Y. Pang, and D. D. Dlott, Chem. Phys. Lett. in press (2003).
[17] Z. Wang, A. Pakoulev, and D. D. Dlott, Science 296 (2002) 2201.
[18] E. J. Heilweil, M. P. Casassa, R. R. Cavanagh, and J. C. Stephenson, J. Chem. Phys. 85 (1986) 5004.
[19] R. Laenen and C. Rauscher, Chem. Phys. Lett. 274 (1997) 63.
[20] S. Woutersen, U. Emmerichs, and H. J. Bakker, J. Chem. Phys. 107 (1997) 1483.
[21] R. Laenen and K. Simeonidis, Chem. Phys. Lett. 299 (1999) 589.
[22] R. Laenen, C. Rauscher, and A. Laubereau, J. Phys. Chem. A 101 (1997) 3201.
[23] L. K. Iwaki and D. D. Dlott, J. Phys. Chem. A 104 (2000) 9101.